

Real time warm pions from the lattice using an effective theory

Sourendu Gupta

*Department of Theoretical Physics, Tata Institute of Fundamental Research,
Homi Bhabha Road, Mumbai 400005, India.*

sgupta@theory.tifr.res.in

Rishi Sharma

*Department of Theoretical Physics, Tata Institute of Fundamental Research,
Homi Bhabha Road, Mumbai 400005, India.*

rishi@theory.tifr.res.in

Lattice measurements provide adequate information to fix the parameters of long distance effective field theories in Euclidean time. Using such a theory, we examine the analytic continuation of long distance correlation functions of composite operators at finite temperature from Euclidean to Minkowski space time. We show through an explicit computation that the analytic continuation of the pion correlation function is possible and gives rise to non-trivial effects. Among them is the possibility, supported by lattice computations of Euclidean correlators, that long distance excitations can be understood in terms of (very massive) pions even at temperatures higher than the QCD cross over temperature.

Keywords: QCD, effective field theory, thermal pion

1. Introduction

The computation of the thermodynamics of quantum field theories is under good control using the Euclidean formulation and non-perturbative lattice computations. Nevertheless the analytic continuation to real time Minkowski quantities remains an open problem, despite decades of attempts to chip away at it. The first attempt to extract a transport coefficient from lattice computations was made more than three decades ago.¹ However, it wasn't until fifteen years later that it was realized that more control was needed on the non-perturbative structure of the spectral density function.² Despite advances in weak-coupling expansions,³ the introduction of new methods,^{4–6} and many lattice computations,^{7–12} the extraction of real-time dynamics at finite temperature from lattice computations is far from becoming a routine measurement. Although some spectacular results have been obtained, this lack of a deeper understanding is a matter of concern. This is partly because there have been improved measurements of many flow variables in heavy-ion collision experiments,^{13,14} and it seems possible to start on the extraction of transport coefficients from data.

While much attention has been focused on the analytic continuation of composite operators which lead to transport coefficients, relatively little has been done about the closely related problem of the analytic continuation of hadron correlation functions (with the exception of heavy quarkonia). Hadrons are composite operators in QCD, and at finite temperature, their Euclidean correlators cannot be connected to Minkowski correlation functions through reflection positivity. Instead of focusing on the most general problem of analytic continuation, our specific discussion will focus on pion properties in real time at finite temperature.

When discussing thermal effects in QCD, it is useful to keep in mind a nomenclature introduced by Smilga.¹⁵ At a temperature above the region of the QCD crossover, *i.e.*, for $T \gg T_{co}$, matter can be considered hot. Well below the crossover, *i.e.*, for $T \ll T_{co}$, he introduced the term lukewarm matter. The region not covered by either name, $T \simeq T_{co}$ we will call warm in this work. We expect that long-distance properties of lukewarm matter should be described in terms of hadrons. Chiral symmetry is broken only by quark masses in hot matter, where hadrons are not expected to be present. Since QCD has a crossover, rather than a sharp phase transition, it is possible that warm matter could be described in terms of either hadrons or quarks, and the more appropriate description is the one which is simpler for any given quantity.

It may be possible, for example, that the correlation function of flavour octet axial currents, at distances much longer than $1/T$, is more easily described in terms of interacting hadron degrees of freedom even for T which is a little larger than T_{co} . Of course this description should become untenable at some $T > T_{co}$. At the same time, it is possible that the equation of state of matter, which is dominated by particles of momentum around T , is more easily described by an interacting quark-gluon liquid. Again, it is possible that this computation remains feasible for some T slightly less than T_{co} but fails badly for a slightly lower temperature. If this happens, then there is nothing contradictory about either description. They could just reflect the complexity of QCD. Rather, tests of such pictures could be in what happens when the quark masses vanish, because then the cross over becomes a phase transition.

At zero temperature there are many ways to capture the physics of chiral symmetry breaking in QCD. At the longest length scales, current algebras relate pion properties to the (broken) Ward identity of chiral charge conservation. Chiral perturbation theory is a systematic effective field theory (EFT) approach that captures an immense amount of hadronic physics at shorter length scales, while also being compatible with current algebra. The non-linear sigma model is another such EFT which captures significant parts of the physics. However, models such as the Nambu-Jona-Lasinio (NJL) model also realize the current algebras, and therefore are interesting approximate low-energy picture of QCD. Quantum hadro-dynamic models try to mimic some aspects of low-energy hadronic physics, and are useful tools in some contexts.

A very early calculation in lukewarm chiral perturbation theory¹⁶ indicated that

the pion mass, m_π , would rise with temperature and the pion decay constant, f_π , would fall. When pursued beyond the leading order,¹⁷ it became clear that the definition of a mass was ambiguous. This led to the notion of a pole mass of a Minkowski propagator, *i.e.*, the energy at which the inverse pion propagator vanishes. An ambiguity also arises in the definition of f_π . When resolved appropriately, the results of the leading order computation could be extended, and qualitative changes in the behaviour of m_π and f_π were seen.

The earliest computation of lukewarm and warm pion properties in the NJL model with two flavours of light quarks¹⁸ obtained Euclidean pion correlators from a one-loop random phase approximation analysis of the Bethe-Salpeter equation. They found that the pion pole mass increases with temperature, and concluded that this was consistent with the behaviour of the screening mass measured on the lattice. Later, a similar computation in the real time formalism¹⁹ for the three flavour NJL model found that the pole mass moved up with temperature. Both these computations were done in the cutoff regularization, with parameters fixed to pion properties at $T = 0$. The second paper made a crucial observation: that predictions can be given in terms of physical quantities by eliminating the cutoff between various predictions in a given model. An NLO computation in the $1/N_c$ expansion of the two-flavour NJL model²⁰ (taken at $N_c = 3$) is the only such computation to report the pion spectral function. Several good reviews exist about the NJL model and its application to physics at finite temperature and density^{21–23}

Another set of approaches has been purely phenomenological, utilizing Lagrangians which express the couplings between many different hadrons. We will subsume all these approaches under the name of Quantum Hadron Dynamics (QHD). A very early computation of pion properties in lukewarm matter²⁴ was done in a model with pions coupled to vector and axial vector mesons with constraints from chiral symmetry for two flavours. The axial anomaly was taken care of, and a full real time computation was done to one-loop order. This work made a very clear and modern analysis of the problem, and reported that screening masses, pole masses, and the dispersion relation barely change in the lukewarm region.

To the best of our knowledge, there is no previous work which specifically addressed the differences between pole and screening masses in the warm region of QCD. This is now accomplished through dual descriptions: both in terms of quarks and pions. Here we report on an EFT model which is specifically engineered for finite temperature and has been seen to successfully reproduce lattice data.²⁵ We give first results on how such an effective field theory can be used to analytically continue Euclidean correlators to real time in the vicinity of the chiral cross over of QCD.

2. The effective field theory model

An EFT is defined with a UV cutoff, Λ , in the momentum, and global symmetries play a major role. All local operators, allowed by symmetry, with mass dimension up

to some order D are included in the EFT Lagrangian. This EFT then should be able to describe the physics of the system for momenta $k \ll \Lambda$ with accuracy $(k/\Lambda)^D$. Because the number of terms is potentially large, so is the number of couplings in the EFT. They are fixed by requiring the EFT to reproduce a sufficient number of measurements. After choosing which measurement to match, if one varies Λ by a small amount, then the values of the fitted parameters also change by a small amount. This is to be interpreted as the analogue of RG running in this cutoff field theory. Once the parameters are fixed, everything else is a prediction of the EFT.

The existence of a special frame where the heat bath is at rest implies a lack of boost invariance in the Lagrangian, as a result of which the global symmetries are of spatial rotations, apart from a $SU(2) \times SU(2)$ chiral-flavour symmetry. We consider a model²⁵ of self-interacting quarks, the Minkowski version of which has the Lagrangian

$$\begin{aligned}
L = & -d^3 T_0 \bar{\psi} \psi + \bar{\psi} \not{\partial}^0 \psi + d^4 \bar{\psi} \not{\nabla} \psi - \frac{d^{61}}{T_0^2} [(\bar{\psi} \psi)^2 + (\bar{\psi} i \gamma_5 \tau^a \psi)^2] \\
& - \frac{d^{62}}{T_0^2} [(\bar{\psi} \tau^a \psi)^2 + (\bar{\psi} i \gamma_5 \psi)^2] - \frac{d^{63}}{T_0^2} (\bar{\psi} \gamma_0 \psi)(\bar{\psi} \gamma^0 \psi) - \frac{d^{64}}{T_0^2} (\bar{\psi} i \gamma_i \psi)(\bar{\psi} i \gamma^i \psi) \\
& - \frac{d^{65}}{T_0^2} (\bar{\psi} \gamma_5 \gamma_0 \psi)(\bar{\psi} \gamma_5 \gamma^0 \psi) - \frac{d^{66}}{T_0^2} (\bar{\psi} i \gamma_5 \gamma_i \psi)(\bar{\psi} i \gamma_5 \gamma^i \psi) \\
& - \frac{d^{67}}{T_0^2} [(\bar{\psi} \gamma_0 \tau^a \psi)(\bar{\psi} \gamma^0 \tau^a \psi) + (\bar{\psi} \gamma_5 \gamma_0 \tau^a \psi)(\bar{\psi} \gamma_5 \gamma^0 \tau^a \psi)] \\
& - \frac{d^{68}}{T_0^2} [(\bar{\psi} i \gamma_i \tau^a \psi)(\bar{\psi} i \gamma^i \tau^a \psi) + (\bar{\psi} i \gamma_5 \gamma_i \tau^a \psi)(\bar{\psi} i \gamma_5 \gamma^i \tau^a \psi)] \\
& - \frac{d^{69}}{T_0^2} [(\bar{\psi} i S_{i0} \psi)(\bar{\psi} i S^{i0} \psi) + (\bar{\psi} S_{ij} \tau^a \psi)^2] \\
& - \frac{d^{60}}{T_0^2} [(\bar{\psi} i S_{i0} \tau^a \psi)(\bar{\psi} i S^{i0} \tau^a \psi) + (\bar{\psi} S_{ij} \psi)^2] .
\end{aligned} \tag{1}$$

where $\not{\partial}^0 = \gamma_0 \partial^0$, also $\not{\nabla} = \gamma_j \partial^j$ with j running over all spatial indices, and τ^a are the generators of flavour $SU(2)$. We use Weinberg's metric conventions.²⁶ This theory is defined with a cutoff, T_0 , which we will choose so that physics at the temperatures of interest can be described by the theory. For later simplicity in writing formulæ, we introduce the notation $\mathcal{N} = 4N_c N_f$ for the number of components of quark fields and $m_0 = d^3 T_0$.

Since the EFT is similar to the Nambu-Jona-Lasinio (NJL) model,²⁷ known techniques²² can be used to first analyze the mean field theory. In the chiral limit, $m_0 = 0$, chiral symmetry is broken spontaneously, a non-vanishing quark condensate, $\langle \bar{\psi} \psi \rangle$, is produced, and a second-order chiral symmetry restoring phase transition (at a temperature that we choose to be T_0) is found. The single combination of the dimension-6 couplings,

$$\lambda = (\mathcal{N} + 2)d^{61} - 2d^{62} - d^{63} + 3d^{64} + d^{65} - 3d^{66} - \frac{3}{2}d^{69} + \frac{3}{2}d^{60}, \tag{2}$$

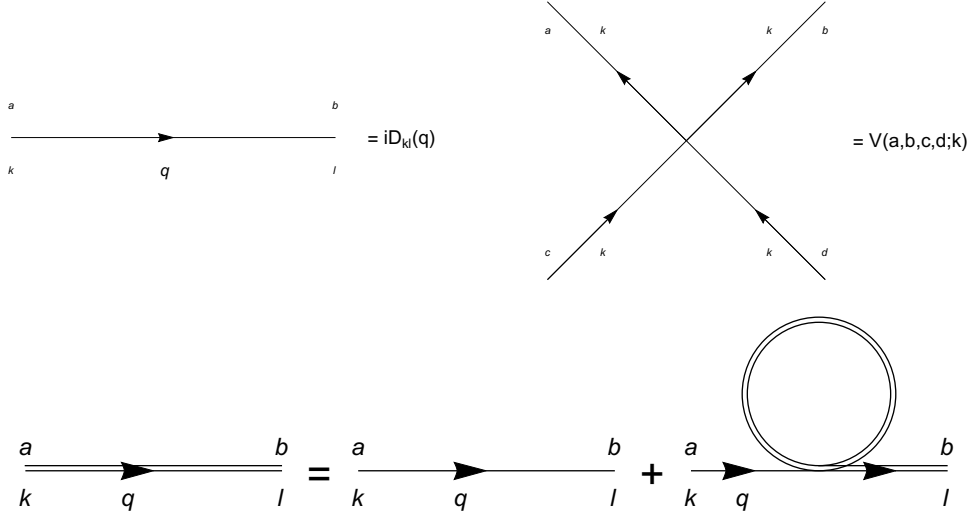


Fig. 1. The Feynman rules for the quark EFT in eq. (1). The thermal propagator $D(q)$ is the 2×2 matrix given in.²⁹ The indices k and l are thermal indices which take values 1 and 2, the rest are composite Dirac, flavour, colour indices. The vertex is diagonal in the thermal index k (which takes values 1 and 2), with $V(a, b, c, d; k) = (-1)^k (2id^{6A}/T_0^2) \Gamma_{ac}^A \Gamma_{bd}^A$, where A runs over all the operator types listed in eq. (1). A diagrammatic representation is also given of the one-loop Dyson-Schwinger equation for the real-time Fermion propagator arising from the Lagrangian in eq. (1).

appears in the subsequent physics that we discuss ^a. In the Euclidean theory these conclusions followed from the computation of the free energy. In real time they come from a self-consistent solution of the one-loop Dyson-Schwinger equation for the quark propagator using real time perturbation theory.^{28,29} In both cases we use dimensional regularization with \overline{MS} subtraction. Since the expressions for the quark condensate are exactly the same in the two computations, the phase structure of the theory can be computed in either the Euclidean or real-time formalism.³⁰

The Euclidean computation has been given in detail in.²⁵ Here we outline how the real time computation proceeds. The Feynman rules for the EFT are shown in Figure 1. Note the fact that the vertex is diagonal in all the thermal indices. Denoting the resummed Dyson-Schwinger propagator as $i\mathcal{D}(q)$, the Neumann series corresponding to the diagrammatic equation in Figure 1 can be written as

$$i\mathcal{D}(q) = iD(q) + iD(q)\Sigma\mathcal{D}(q) \quad (3)$$

The very simple structure of the vertex factor then allows us to decouple the equations for \mathcal{D}_{11} . This forces all the internal quark lines in the superdaisy graphs to be D_{11} . As a result, the computation reduces to well known pieces.^{27,30} The one-loop

^aThis formula corrects an earlier typographical error.²⁵

self-energy σ , whose iteration would give the Σ in eq. (3), is given by

$$\sigma_{lk} = - \sum_A \frac{2id^{6A}}{T_0^2} \int \frac{d^4p}{(2\pi)^4} [\Gamma_{mn}^A \{D_{11}(p)\}_{nm} \Gamma_{lk}^A - \Gamma_{ln}^A \{D_{11}(p)\}_{nm} \Gamma_{mk}^A]. \quad (4)$$

The integral gives zero when the numerator has a linear term in the momentum p . Therefore, the result is diagonal in spinor-flavour-colour indices. Performing the traces, we get exactly the linear combination of the couplings shown in eq. (2). Furthermore, the result is real. Then putting this into the Dyson-Schwinger resummation, one obtains a self-consistency equation for the Fermion mass which is exactly the same as the gap equation in Euclidean space.

At finite m_0 , the quark mass explicitly breaks chiral symmetry. Nevertheless, a remnant of spontaneous chiral symmetry breaking appears as a large value of the condensate, giving an effective quark mass $m = m_0 + \Sigma$, where $\Sigma = 2\lambda\langle\bar{\psi}\psi\rangle/T_0^2$. As the temperature is increased, Σ crosses over to a small value. This is exactly what was found in the Euclidean computation.²⁵

The fixing of the parameters in the action of eq. (1) was done by matching one-loop expressions for the axial current correlators to lattice measurements.³² The process was simple; since the axial symmetry is broken, small fluctuations around the mean field have the quantum numbers of the pion. These fluctuations can be parametrized by the following field redefinition when using a Hubbard-Stratanovich transformation,

$$\psi \rightarrow \exp \left[\frac{i\pi\gamma^5}{2f} \right] \psi \quad (5)$$

with a three component field $\pi = \pi^a \tau^a$, and a constant f with the dimension of mass. We will show elsewhere that this transformation correctly takes into account exchange effects which capture the correct value of λ given in eq. (2). Introducing this parametrization into the quark action and expanding to second order in π gives a coupled model of quarks and mesons

$$L_c = -\bar{\psi} \left[d^3 T_0 \left(1 + i\gamma^5 \frac{\pi}{f} - \frac{\pi^2}{2f^2} \right) - \not{\partial} - \frac{i}{2f} \gamma^5 \not{\partial} \pi \right] \psi + \dots \quad (6)$$

where $\not{\partial} = \not{\partial}^0 + d^4 \not{\nabla}$, and the terms of dimension-6 and higher have not been written out. The pion appears as an auxiliary field, and hence has no kinetic term in L_c . After integrating over the quark fields, an effective pion action was obtained, with parameters of the action expressed in terms of the parameters in the quark Lagrangian.

In the chiral limit the axial vector current is conserved; the conservation law is broken only by the parameter d^3 in the action. Using the one-loop version of the PCAC relation at finite temperature, the long-distance static axial current correlator could be parametrized in terms of the coupling constants d^3 and d^4 . The convention that T_0 is the chiral transition temperature T_c fixes λ , and the value of T_0 was then inferred from matching the cross over temperature, T_{co} , at finite m_0 simultaneously with the matching of axial current correlators.²⁵

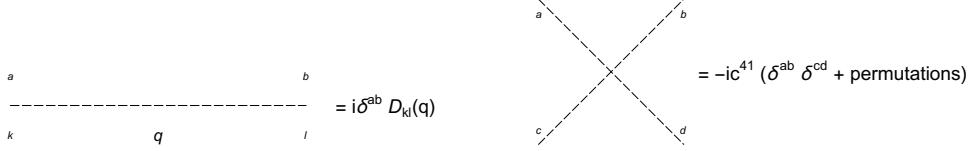


Fig. 2. The Feynman rules for pions generated by the Lagrangian in eq. (7). The flavour indices are a, b, c, d . The indices k and l which run over 1 and 2 refer to the thermal components of fields.

3. Analytic continuation of correlation functions

The specific question that we ask here is how the parameters which govern the long-distance part of the pion correlation function can be analytically continued to real time. Since we have a EFT which is written in terms of the pions, it should be a simple matter to use it to do the continuation. We present this here.

The Minkowski Lagrangian for the pion EFT has the form

$$L_f = -\frac{1}{2}c^2 T_0^2 \pi^2 + \frac{1}{2}(\partial_0 \pi)^2 - \frac{1}{2}c^4 (\nabla \pi)^2 - \frac{c^{41}}{8} \pi^4. \quad (7)$$

which includes all terms of dimension up to 4. In the rest of this paper we will assume that all the dimensionless coupling parameters have exactly the value that they have with the one-loop matching described in the previous section, and use the shorthand notation $\mathbf{m}^2 = c^2 T_0^2$. The pole mass computed to higher loop order in the pion theory will be referred to as m_π .

We need to compute only the 11 component of the 2×2 thermal correlation function because we are interested in external pion states.²⁸ At tree level the pion correlation function is give by

$$\mathcal{D}_{11}^\pi(q) = [q_0^2 - c^4 |\mathbf{q}|^2 - \mathbf{m}^2 + i\epsilon]^{-1} + 2\pi i n_B(q_0) \delta(q_0^2 - c^4 |\mathbf{q}|^2 - \mathbf{m}^2), \quad (8)$$

where n_B denotes the Bose distribution function. The spectral function,

$$\rho(q^0, |\mathbf{q}|) = iD_R(q^0, |\mathbf{q}|) - iD_A(q^0, |\mathbf{q}|), \quad (9)$$

which is the imaginary part of the causal correlator, has support only on the “acoustic shell” $q_0^2 = c^4 |\mathbf{q}|^2 - \mathbf{m}^2$. This simple spectral function means that there is no special subtlety in analytic continuation from spacelike to timelike momenta. Since the spacelike region is captured in Euclidean lattice computations, this means that the values of c^2 , c^4 , and c^{41} are those extracted by matching lattice data.²⁵

The Feynman rules for the pion theory are given in Figure 2. Note the simple form of the vertex which was also pointed out earlier for the quark computation; the vertex forces all fields connected to it to be either type 1 or type 2. The one-loop correction is given in Figure 3. The cutting rules²⁸ at finite temperature can be understood as dividing vertices into two categories, circled and uncircled, and cutting the propagators which connect two different types of vertices. Since there is only one vertex in this diagram, no cuts are possible. As a result, the diagram gives a purely real contribution. The flavour indices at the vertex contract in two

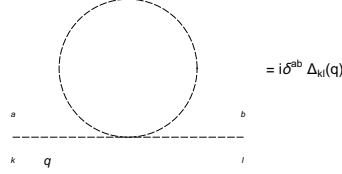


Fig. 3. The Feynman diagram for the pion correlation function up to one loop order. The external momentum is q , and the external flavour indices are a, b .

ways. The contraction $\delta^{ab}\delta^{cc}$ gives $(N_f^2 - 1)/2$, and $\delta^{ac}\delta^{cb}$ gives unity. As a result, the one-loop self-energy can be written as

$$\delta m_\pi^2 = \frac{i}{2} c^{41} (1 + N_f^2) \int \frac{d^4 k}{(2\pi)^4} D_{11}^\pi(k). \quad (10)$$

Since this is independent of q , it gives no contribution to c^4 , c^{41} or f . With the $\overline{\text{MS}}$ regularization eq. (10) gives

$$\delta m_\pi^2 = \frac{c^{41}}{2(c^4)^{3/2}} (1 + N_f^2) \left[\frac{\mathbf{m}^2}{16\pi^2} \left\{ \log \left(\frac{\mathbf{m}^2}{c^4 M^2} \right) - 1 \right\} + \int \frac{d^3 k}{E_k (2\pi)^3} n_B(E_k) \right], \quad (11)$$

where we have scaled c^4 out of the integral, and then defined $E_k = \sqrt{k^2 + \mathbf{m}^2}$. The choice of the renormalization point, M , is arbitrary; we will choose it to be the same as in the quark theory. The pole mass is then $m_\pi^2 = \mathbf{m}^2 + \delta m_\pi^2$. Proceeding to the Dyson-Schwinger superdaisy resummation^{22,31} is straightforward and follows the same lines as in the quark case. There are no complications due to spinor indices, and the resummation of the result in eq. (11) is straightforward; one replaces \mathbf{m}^2 on the right hand side by $\mathbf{m}^2 + \delta_\pi^2$ and solves the equation numerically for δm_π .

The results for the pole mass are shown in Figure 4. One sees that in the whole warm region of QCD, thermal effects are important, since the pion pole mass differs significantly from the pion mass at zero temperature, and is actually smaller. We note that the pole mass rises as the temperature approaches T_{co} . We have continued the computation to temperatures slightly above T_{co} , because, as discussed earlier, a cross over does not necessarily prevent a hadronic description from holding above this temperature. Whether this is in agreement with QCD is discussed next.

Static correlators fall off with distance exponentially with the Debye screening mass, $M_\pi = m_\pi/\sqrt{c^4}$. For real-time dynamic correlators, the dispersion relation for small q is $E = m_\pi + |\mathbf{q}|^2/(2M_K)$, where the rest mass is exactly the pole mass, but the kinetic energy involves a kinetic mass, which is given by $M_K = m_\pi/c^4$. Results for both are shown in Figure 5. Note that the one-loop result gives an improved description of the lattice measurements of M_π ³² even at temperatures a little above T_{co} . We note that to this order, the appropriate values of c^4 and f remain as obtained from Euclidean lattice computations. We have more remarks on this in the next section.

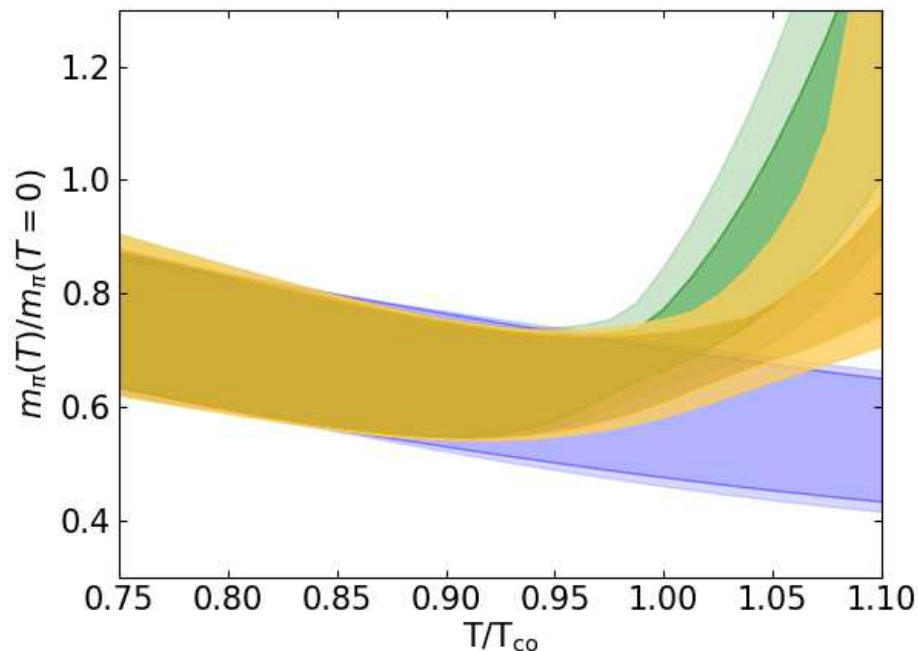


Fig. 4. The pion pole mass as a function of temperature. In warm QCD, the pion is strongly affected by temperature. The band in blue shows the tree level, in green the one loop corrected, and in gold the one loop Dyson-Schwinger resummed result. The darker inner part of each band is the region allowed by the statistical uncertainties in parameters²⁵ for $M = 1.6\pi T_0$, and the lighter outer part is the result of a variation in the renormalization scale $1.2 \leq M/(\pi T_0) \leq 2.0$. The pion mass at $T = 0$ is taken from a lattice computation with the same Lagrangian and parameters as the finite temperature computation to which the matching is performed.

4. Issues

The agreement of screening masses measured on the lattice with the one loop values raises several interesting physics questions. Since the pole mass of the pion at finite temperature is smaller than the pion mass at $T = 0$ (see Figure 4) earlier computations in chiral perturbation theory^{16,17} and the NJL model^{18,19} must differ in some piece of the physics. We believe it is the fact that the breaking of Lorentz invariance allows the pion kinetic term to take on a non-trivial value of c^4 . This is constrained by lattice data, and gives a difference between the pole and screening masses. Since it varies extremely rapidly in the warm region, it is important. From Figure 4 it seems that $m_\pi(T)/m_\pi(T=0)$ could become closer to unity at smaller temperature. Whether or not it exceeds unity at some intermediate temperature in the lukewarm region remains an open question.

The other question is even more intriguing. Until what temperature can the pion

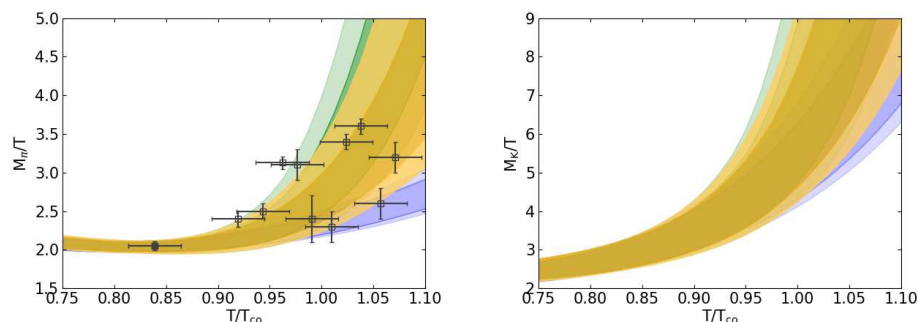


Fig. 5. The pion screening mass (left) and kinetic mass (right). The band in blue shows the tree level, in green the one loop corrected, and in gold the one loop Dyson-Schwinger resummed result. The darker inner part of each band is the result of the statistical uncertainties in parameters,²⁵ and the lighter outer part is the result of a variation in M/T_0 . The lattice measurements of the screening mass³² are also shown. The filled point is the only screening mass which was used in the extraction of EFT parameters; the rest are predictions.

theory be used? Pion fields were introduced to capture small fluctuations around a local minimum of the free energy. In the chiral limit this can no longer make sense beyond T_c . When there is a cross over, the symmetry broken minimum does not vanish abruptly. However, at some temperature the “radial” fluctuations, corresponding to a scalar mode, can no longer be neglected, and the pure pion theory cannot make sense. It has been seen in lattice computations^{33,34} that pion and scalar masses remain distinct at temperatures lower than $1.1T_{co}$. This could be the reason why the pion theory seems to explain physics at temperature higher than T_{co} , albeit with a pion pole mass which rapidly increases. There is a range of temperatures where one has chiral symmetry restoration but long-distance correlations are still mediated by a hadronic excitation, namely a very massive pion.

One could turn the question around, and ask whether the compositeness of the pion should be expected show up in the computation of correlation functions at long-distances. A computation in which compositeness was assumed to show up was reported long back in the large N Gross-Neveu model at finite temperature.³⁵ It was also reported that similar results are obtained when pion correlators are computed using the quark EFT to one loop,³⁶ except that the Gell-Mann-Oakes-Renner relation was satisfied (the difference could be due to the fact that a $\overline{\text{MS}}$ regularization, which preserves symmetries, was used in the EFT computation). However, there is ample observational evidence in a variety of physical systems that long-distance correlation functions of Goldstone bosons do not see the underlying compositeness. The most straightforward experimental evidence for this is in Andreev reflections: if an electron is incident on a normal-superconducting boundary, a hole is reflected from the interface, and only a Cooper pair propagates inside the superconductor. This happens not only at $T = 0$ but also at finite temperature, as long as the super-

conducting gap is large enough. There is no violation of decoupling theorems. What this means for QCD is that one should expect that the long-distance correlators of pions can be computed in the pion EFT, as long as the pion remains the lightest mode around the symmetry-broken minimum.

Nevertheless, there is some interesting, and generic, physics which is not captured in the computation presented here. A collection of particles in a heat bath scatter off each other, giving rise to quite non-trivial spectral functions. This is not seen in the one loop result, for the simple reason that the external momentum does not enter the loop. It is clear that two loop computations will give more interesting, and generic, structures. In particular, the dependence on external momentum will modify all couplings as well as f , and the corrections could differ in the spacelike and timelike regimes. Such a computation is currently underway, and the results will be reported soon.

References

1. F. Karsch and H. W. Wyld, Phys. Rev. D **35**, 2518 (1987).
2. G. Aarts and J. M. Martinez Resco, JHEP **0204**, 053 (2002) [hep-ph/0203177].
3. P. B. Arnold, G. D. Moore and L. G. Yaffe, JHEP **0011** 001 (2000) [hep-ph/0010177], JHEP **0305**, 051 (2003) [hep-ph/0302165].
4. M. Asakawa, T. Hatsuda and Y. Nakahara, Prog. Part. Nucl. Phys. **46** (2001) 459 [hep-lat/0011040].
5. S. Gupta, Phys. Lett. B **597** (2004) 57 [hep-lat/0301006].
6. M. Kitazawa, T. Iritani, M. Asakawa and T. Hatsuda, Phys. Rev. D **96** (2017) no.11, 111502 [arXiv:1708.01415 [hep-lat]].
7. S. Sakai, A. Nakamura and T. Saito, Nucl. Phys. A **638**, 535 (1998) [hep-lat/9810031].
8. F. Karsch, E. Laermann, P. Petreczky, S. Stickan and I. Wetzorke, Phys. Lett. B **530** (2002) 147 [hep-lat/0110208].
9. M. Asakawa and T. Hatsuda, Phys. Rev. Lett. **92** (2004) 012001 [hep-lat/0308034].
10. S. Datta, F. Karsch, P. Petreczky and I. Wetzorke, Phys. Rev. D **69** (2004) 094507 [hep-lat/0312037].
11. H. B. Meyer, Phys. Rev. Lett. **100** (2008) 162001 [arXiv:0710.3717 [hep-lat]].
12. O. Philipsen and C. Schäfer, JHEP **1402** (2014) 003 [arXiv:1311.6618 [hep-lat]].
13. J. Jia [ATLAS Collaboration], J. Phys. G **38** 124012 (2011) [arXiv:1107.1468 [nucl-ex]].
14. G. Aad *et al.* [ATLAS Collaboration], JHEP **1311**, 183 (2013) [arXiv:1305.2942 [hep-ex]].
15. A. V. Smilga, Phys. Rept. **291**, 1 (1997) [hep-ph/9612347].
16. J. Gasser and H. Leutwyler, Phys. Lett. B **184**, 83 (1987).
17. D. Toublan, Phys. Rev. D **56**, 5629 (1997) [hep-ph/9706273].
18. T. Hatsuda and T. Kunihiro, Phys. Lett. B **185**, 304 (1987).
19. M. F. M. Lutz, S. Klimt and W. Weise, Nucl. Phys. A **542**, 521 (1992). doi:10.1016/0375-9474(92)90256-J
20. D. Muller, M. Buballa and J. Wambach, Phys. Rev. D **81**, 094022 (2010) [arXiv:1002.4252 [hep-ph]].
21. U. Vogl and W. Weise, Prog. Part. Nucl. Phys. **27**, 195 (1991).
22. S. P. Klevansky, Rev. Mod. Phys. **64**, 649 (1992). doi:10.1103/RevModPhys.64.649
23. T. Hatsuda and T. Kunihiro, Phys. Rept. **247**, 221 (1994) [hep-ph/9401310].

24. C. Song, Phys. Rev. D **49**, 1556 (1994).
25. S. Gupta and R. Sharma, Phys. Rev. D **97**, no. 3, 036025 (2018) [arXiv:1710.05345 [hep-ph]].
26. S. Weinberg, “The Quantum Theory of Fields: Volume 2, Modern Applications”, Cambridge University Press, Cambridge, 1996.
27. Y. Nambu and G. Jona-Lasinio, Phys. Rev. **122** (1961) 345. Y. Nambu and G. Jona-Lasinio, Phys. Rev. **124** (1961) 246.
28. R. L. Kobes, G. W. Semenoff and N. Weiss, Z. Phys. C **29**, 371 (1985).
29. R. L. Kobes and G. W. Semenoff, Nucl. Phys. B **260**, 714 (1985).
30. N. P. Landsman and C. G. van Weert, Phys. Rept. **145**, 141 (1987).
31. L. Dolan and R. Jackiw, Phys. Rev. D **9**, 3320-3341 (1974).
32. B. B. Brandt, A. Francis, H. B. Meyer and D. Robaina, Phys. Rev. D **90** (2014) no.5, 054509 [arXiv:1406.5602 [hep-lat]].
33. S. Gupta and N. Karthik, Phys. Rev. D **87**, no.9, 094001 (2013) [arXiv:1302.4917 [hep-lat]].
34. A. Bazavov, S. Dentinger, H. T. Ding, P. Hegde, O. Kaczmarek, F. Karsch, E. Laermann, A. Lahiri, S. Mukherjee, H. Ohno, P. Petreczky, R. Thakkar, H. Sandmeyer, C. Schmidt, S. Sharma and P. Steinbrecher, Phys. Rev. D **100** (2019) no.9, 094510 [arXiv:1908.09552 [hep-lat]].
35. S. Z. Huang and M. Lissia, Phys. Rev. D **53**, 7270 (1996) [hep-ph/9509360].
36. S. Gupta and R. Sharma, [arXiv:1904.11265 [hep-ph]].